

Optical polarimetric study of open clusters: Distribution of Interstellar matter towards NGC 654

Biman J. Medhi^{1*}, Maheswar. G^{1,2}, J. C. Pandey¹, T. S. Kumar¹ and Ram Sagar¹

¹*Aryabhata Research Institute of Observational Sciences, Manora Peak, Nainital - 263 129, India*

²*Korea Astronomy and Space Science Institute 61-1, Hwaam-dong, Yuseong-gu, Daejeon, Republic of Korea 305-348*

ABSTRACT

We present new B , V and R linear polarimetric observations for 61 stars towards the region of the young open cluster NGC 654. In this study we found evidence for the presence of at least two layers of dust along the line of sight to the cluster. The distances to the two dust layers are estimated to be ~ 200 pc and ~ 1 kpc which are located much closer to the Sun than the cluster (~ 2.4 kpc). Both the dust layers have their local magnetic field orientation nearly parallel to the direction of the Galactic plane. The foreground dust layer is found to have a ring morphology with the central hole coinciding with the center of the cluster. The foreground dust grains are suggested to be mainly responsible for both the observed differential reddening and the polarization towards the cluster.

Key words: polarization- dust, extinction- open clusters and associations:individual:
NGC 654

1 INTRODUCTION

The wavelength dependence of interstellar extinction and polarization provides constraints on the characteristics of interstellar grains. Interstellar polarization strongly varies with wavelength (Serkowski, Mathewson & Ford 1975; Wilking *et al.* 1980). In particular, the wavelength of maximum interstellar polarization (λ_{max}) is thought to be related to the total-to-selective extinction (R_V) as $R_V = (5.6 \pm 0.3)\lambda_{max}$ (Whittet & van Breda 1978).

* E-mail: biman@aries.ernet.in

The polarization of background starlight has been used for nearly five decades to probe the magnetic field direction in the interstellar medium (ISM). The observed polarization is believed to be caused by the dichroic extinction of background starlight passing through the concentrations of aligned and elongated dust grains along the line of sight. Although there is no general consensus on which is the dominant grain alignment mechanism (Lazarian, Goodman & Myers 1997), it is generally believed that the elongated grains tend to become aligned to the local magnetic field with their shortest axis parallel to the field. For this orientation, the observed polarization vector is parallel to the plane-of-sky projection of a line-of-sight-averaged magnetic field (Davis & Greenstein 1951).

Young open clusters are very good candidates to carry out the polarimetric observations because of available knowledge on their physical parameters like distance, membership probability (M_p) and colour excess ($E(B - V)$). This would enable us to undertake a meaningful study of foreground interstellar dust.

As a part of an observational programme to carry out polarimetric observations of young open clusters towards anti-galactic center direction ($l = 120^\circ - 180^\circ$) to investigate the properties like magnetic field orientation, λ_{max} , maximum polarization (P_{max}), etc., we observed two young open cluster IC 1805 (Medhi et al. 2007) and NGC 654. In this paper we present the results obtained from our study on NGC 654. The young open cluster NGC 654 (*R.A.* (*J2000*) : $01^h44^m00^s$, *Dec* (*J2000*) : $+61^\circ 53^m 06^s$; $l = 129.08^\circ$, $b = -00.36^\circ$) in Cassiopeia has been classified as Trumpler class II2r by Lyngå (1984). The post-main-sequence stars in NGC 654 reveal an age of $\sim 10 - 30$ Myr for the cluster, whereas the pre-main-sequence stars indicate an age of $\sim 1 - 10$ Myr (Pandey et al. 2005). The value of $E(B - V)$ across the cluster varies in the range $\sim 0.7 - 1.2$ mag (Joshi & Sagar 1983; Phelps & Janes 1994). A distance modulus of 14.7 ± 0.10 which corresponds to 2.41 ± 0.11 kpc (for a normal reddening law) is estimated for the cluster (Pandey et al. 2005).

First polarimetric measurements of the stars towards NGC 654 were made by Samson (1976) with plates using IIA0 emulsion (IIA0 emulsion has a red cutoff similar to Johnson B band). Samson (1976) found certain stars to be very conspicuous because they differed in magnitude or direction of polarization, or both, from the surrounding stars. The star #37 for e.g., was unusual in both the magnitude and direction of polarization. He suggested a dust cloud partially obscuring the area to be the reason. The general direction of polarization was found to be parallel to the Galactic magnetic field. Recently, Pandey et al.(2005) observed 7 stars in the vicinity of NGC 654. Of these 7 stars, 4 of them with higher membership

Table 1. Observed polarized and unpolarized standard stars

| Filter | Polarized Standard | | | | Unpolarized Standard | |
|--------|-------------------------|---------------------------------|----------------------|---------------------------------|----------------------|---------|
| | $P \pm \epsilon(\%)$ | $\theta \pm \epsilon(^{\circ})$ | $P \pm \epsilon(\%)$ | $\theta \pm \epsilon(^{\circ})$ | $q(\%)$ | $u(\%)$ |
| | Schmidt & Elston (1992) | | This work | | This work | |
| | <u>Hiltner-960</u> | | | | <u>HD21447</u> | |
| B | 5.72 ± 0.06 | 55.06 ± 0.31 | 5.62 ± 0.20 | 54.65 ± 1.04 | 0.019 | 0.011 |
| V | 5.66 ± 0.02 | 54.79 ± 0.11 | 5.70 ± 0.14 | 53.37 ± 0.08 | 0.037 | - 0.031 |
| R | 5.21 ± 0.03 | 54.54 ± 0.16 | 5.20 ± 0.06 | 54.80 ± 0.38 | - 0.035 | - 0.039 |
| | <u>HD 204827</u> | | | | <u>HD12021</u> | |
| B | 5.65 ± 0.02 | 58.20 ± 0.11 | 5.72 ± 0.09 | 58.60 ± 0.49 | - 0.108 | 0.071 |
| V | 5.32 ± 0.02 | 58.73 ± 0.08 | 5.35 ± 0.03 | 60.10 ± 0.20 | 0.042 | - 0.045 |
| R | 4.89 ± 0.03 | 59.10 ± 0.17 | 4.91 ± 0.20 | 58.89 ± 1.20 | 0.020 | 0.031 |
| | <u>BD+64°106</u> | | | | <u>HD14069</u> | |
| B | 5.51 ± 0.09 | 97.15 ± 0.47 | 5.46 ± 0.10 | 99.40 ± 0.50 | 0.138 | - 0.010 |
| V | 5.69 ± 0.04 | 96.63 ± 0.18 | 5.48 ± 0.11 | 97.09 ± 0.12 | 0.021 | 0.018 |
| R | 5.15 ± 0.10 | 96.74 ± 0.54 | 5.20 ± 0.02 | 97.35 ± 0.18 | 0.010 | - 0.014 |
| | <u>HD 19820</u> | | | | <u>G191B2B</u> | |
| B | 4.70 ± 0.04 | 115.70 ± 0.22 | 4.81 ± 0.20 | 113.49 ± 0.19 | 0.072 | - 0.059 |
| V | 4.79 ± 0.03 | 114.93 ± 0.17 | 4.91 ± 0.10 | 114.55 ± 0.20 | - 0.022 | - 0.041 |
| R | 4.53 ± 0.03 | 114.46 ± 0.17 | 4.70 ± 0.13 | 113.88 ± 0.21 | - 0.036 | 0.027 |

probability (M_P) showed relatively large polarization (3.03 to 4.47%) and a mean position angle $PA_V \simeq 94^{\circ}$ in V filter. The two non-member stars showed relatively small polarization ($\sim 2\%$) and a mean $PA_V \simeq 105^{\circ}$. The remaining star # 57 with $M_P = 0.90$ (Stone 1977) was identified as a non-member (Sagar & Yu 1989) also showed values (2% & 102°) similar to those of two non-member stars. From their multi-wavelength study, they concluded that the dust grains associated with NGC 654 are smaller than those associated with the general interstellar medium.

In this paper, we present the results of polarimetric measurements made for 61 stars in B, V and R photometric bands towards NGC 654 (brighter than $V \simeq 17$ mag). Of the 61 stars observed, 8 of them have high membership probability ($M_P \geq 0.7$). The paper is organized as following: in section 2 we present observations; the results and discussion are presented in section 3 and in section 4 we conclude with a summary.

2 OBSERVATIONS

The optical imaging polarimetric observations of the two fields (centered at $R.A. : 01^h43^m19^s$, $Dec : +61^{\circ}51^m31^s$ and $R.A. : 01^h43^m56^s$, $Dec : +61^{\circ}57^m48^s$) in NGC 654 were carried out on 27th and 28th December, 2006 using ARIES Imaging Polarimeter (AIMPOL; Medhi *et al.* 2007, Rautela, Joshi & Pandey 2004) mounted on the Cassegrain focus of the 104-cm Sampurnanand telescope of ARIES, Nainital in B, V and R ($\lambda_{B_{eff}}=0.440 \mu m$, $\lambda_{V_{eff}}=0.550 \mu m$ and $\lambda_{R_{eff}}=0.660 \mu m$) photometric bands. The imaging was done by using a $TK 1024 \times 1024$

pixel² CCD camera. Each pixel of the CCD corresponds to 1.7 arcsec and the field of view is ~ 8 arcmin diameter on the sky. The FWHM of the stellar image varies from 2 to 3 *pixel*. The read out noise and gain of the CCD are $7.0 e^-$ and $11.98 e^-/\text{ADU}$, respectively. The fluxes for all of our programme stars were extracted by aperture photometry after the bias subtraction in the standard manner using IRAF. The detail descriptions about the AIM-POL, data reduction and calculations of polarization, position angle are given in Medhi *et al.* (2007).

Standard stars for null polarization and for the zero point of the polarization position angle were taken from Schmidt & Elston (1992). The observed degree of polarization ($P\%$) and position angle (θ) for the polarized standard stars and their corresponding values from Schmidt & Elston (1992) are given in Table 1. The observed values of $P\%$ and θ are in good agreement with those given in Schmidt & Elston (1992) within the observational errors. The observed normalized stokes parameters $q\%$ and $u\%$ for standard unpolarized stars (Schmidt & Elston 1992) are also given in Table 1. The average value of instrumental polarization is found to be $\sim 0.04\%$.

The ordinary and extraordinary images of each source in the CCD frame is separated by 27 *pixels* along the north-south direction on the sky plane. Due to the lack of a grid, placed to avoid the overlapping of ordinary image of one source with the extraordinary of an adjacent one located 27 *pixels* away along the north-south direction, we avoided the central crowded portion of the cluster. However, the fields are chosen in such a manner to include maximum number of member stars. We also had a large number of sources which are not members but are present in the fields observed. All the sources were manually checked and rejected in case of an overlapping. But background at any location of the observed field gets doubled due to this overlapping and may have significant effect if the background has variation within 27 *pixels* (e.g., presence of reflection nebulosity). One star, BD+61 315, is found to be associated with a faint nebulosity. We suspect that, due to the lack of grid in our polarimeter, the reflection nebulosity may have contributed polarized light over the aperture used for the photometry. We discuss this issue in section 3.

3 RESULTS & DISCUSSION

Our polarimetric results are presented in the Table 2. Column 2 gives the star identification as given by Phelps & Janes (1994). Instrumental magnitudes obtained in V filter are given

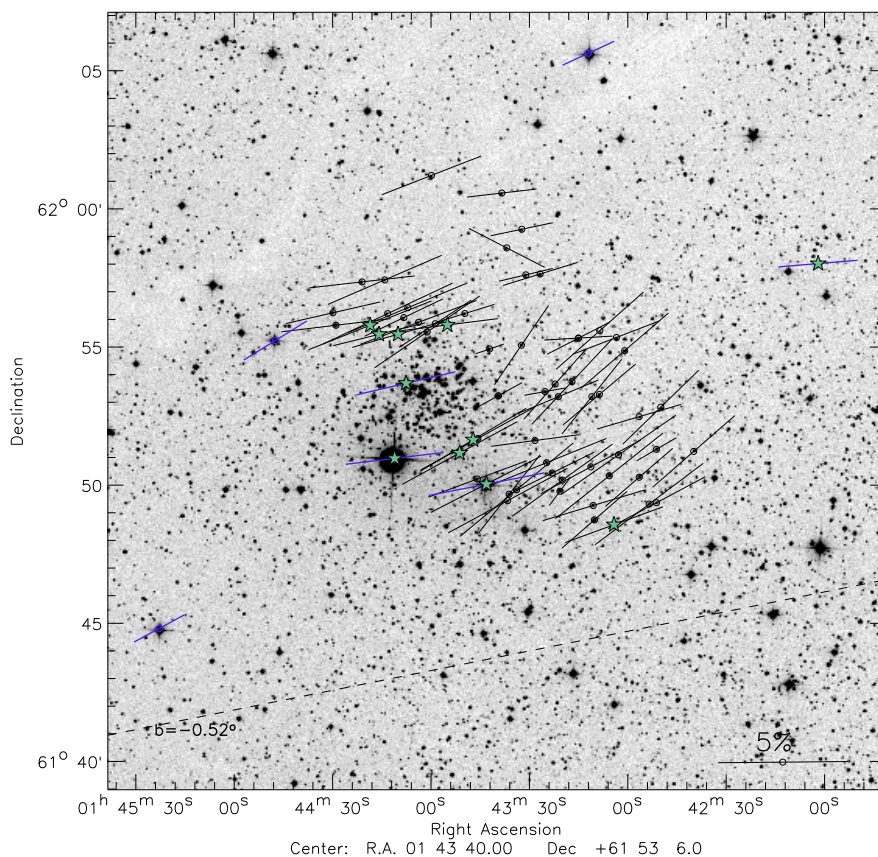


Figure 1. The $28' \times 28'$ R-band DSS image of the field containing NGC 654, reproduced from Digitized Sky Survey. The position angles, in the equatorial coordinate system, are measured from the north, increasing eastward. The polarization vectors are drawn with the star as the center. Length of the polarization vector is proportional to the percentage of polarization P_V and it is oriented parallel to the direction corresponding to the observed polarization position angle θ_V . A vector with a P of 5% is shown for reference. The dashed line represents the Galactic parallel at $b = -0.52^\circ$. Stars with $M_P \geq 0.70$ are identified with closed star symbols in green colour. Polarization vectors of seven stars observed by Pandey et al. (2005) are shown in blue colour.

in column 3. The measured values of polarization P (in %) and the corresponding error ϵ (in %) in B, V and R filters are given in columns 4, 6, & 8, respectively. The polarization position angle (of the \mathbf{E} vector) θ (in $^\circ$) and the corresponding error ϵ (in $^\circ$) in B, V and R filters are given in columns 5, 7 & 9, respectively. The position angles in the equatorial coordinate system are measured from the north increasing eastward. Columns 10 & 11 represent $E(B - V)$ (Joshi & Sagar 1983) and the membership probabilities (M_P) (Stone 1977; Joshi & Sagar 1983; Huestamendia, Rio & Mermilliod 1993), respectively. Stars with $M_P \geq 0.70$ are considered as cluster members in this study.

In Table 3, we present previous polarization measurements of stars in the direction of NGC 645 carried out by Samson (1976) and Pandey et al. (2005). Samson (1976) observed 14 stars in the direction of NGC 654 using plates with IIA0 emulsion. The IIA0 emulsion has a red cutoff similar to Johnson B band. The limiting magnitude was $B = 15$ mag. In column

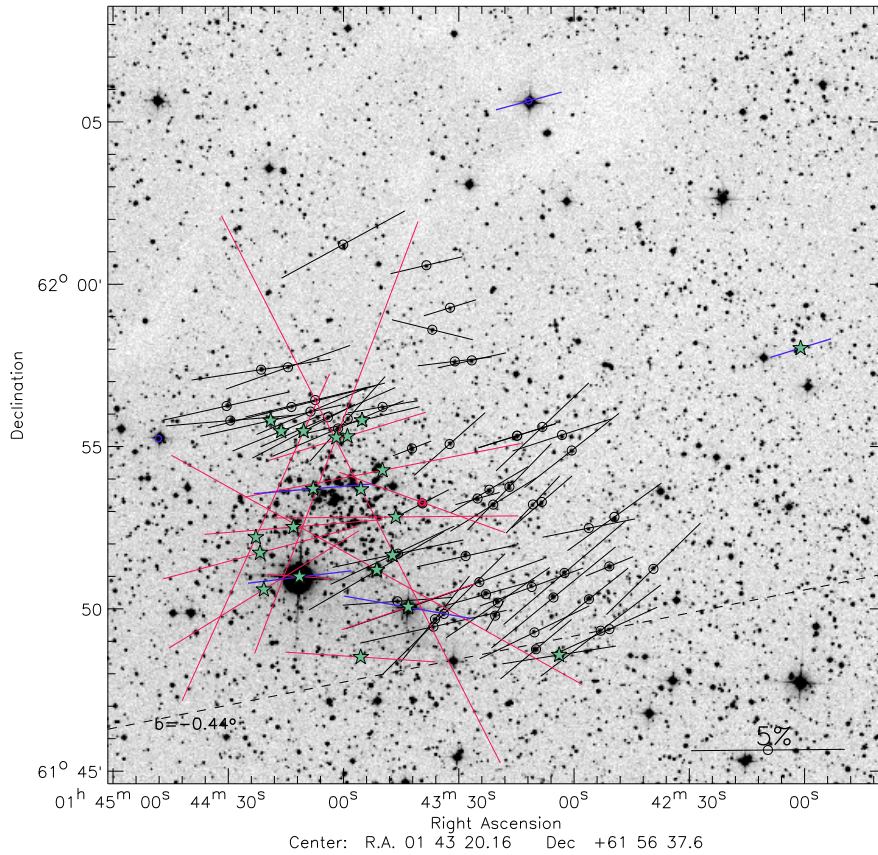


Figure 2. Same as in Figure 1 but for P_B and θ_B . Results for 14 stars observed by Samson (1976) using Ila0 emulsion plates (which has a red cutoff similar to Johnson B band) are shown using vectors drawn in red. Three out of five stars for which Pandey et al. (2005) had B band measurements are also shown using vectors in blue.

1, we give the identification numbers which are adopted from Samson (1976) and Pandey et al. (2005). Columns 2, 3, 4, 5, 6, 7, 8, & 9 give $P\%$ & θ in B, V, R & I filters, respectively. The errors of measurements are given in parenthesis wherever available. Samson (1976) gives polarization in magnitudes (p). We converted p to $P\%$ using the relation $P\% = 46.05p$ (Whittet 1992). The position angles given by Samson (1976) are w.r.t the east, as deduced from the star #54. We transformed the values to w.r.t the north. In column 10 we give the membership probabilities of stars obtained from Stone (1977).

The sky projection of the V-band polarization vectors for the 61 stars observed by us in NGC 654 are shown in Figure 1 (R band image is reproduced from Digitized Sky Survey). The polarization vectors are drawn with the observed stars at the center. The length of the polarization vector is proportional to the percentage of polarization in V band (P_V) and it is oriented parallel to the direction of corresponding observed polarization position angle in V band (θ_V). The dashed line represents the Galactic parallel at $b = -0.52^\circ$ inclined at $\sim 100^\circ$ w.r.t the north. The stars with $M_P \geq 0.70$ are identified using closed star symbols

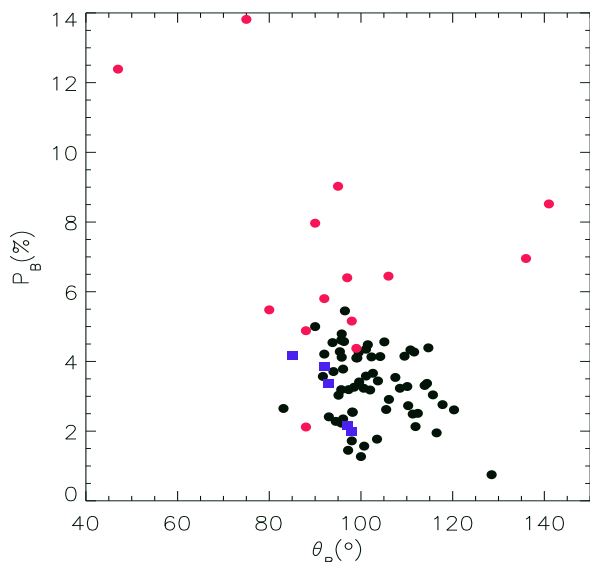


Figure 3. The P_B vs. θ_B plot for 61 stars observed by us in the direction of NGC 654 are shown using black filled circles. Results of stars observed by Samson (1976) and Pandey et al. (2005) are shown using filled red circles and blue squares.

in green. Polarization vectors for 7 stars observed by Pandey et al. (2005) are also shown in blue colour. Clearly, there exist stars with vectors (a) distributed about the Galactic plane and (b) slightly greater than the Galactic plane (especially those located to the west and to the south-western regions of the cluster). This indicates that the dust grains along the line of sights are mostly aligned by a magnetic field which is nearly parallel to the direction of the Galactic Disk. But a second component of magnetic field which is slightly inclined to the Galactic Disk could also be present along the line of sights of stars showing steeper angles.

In Figure 2 we present the sky projection of the B-band polarization vectors for the 61 stars observed by us in NGC 654 (vectors in black colour) along with the results from Samson (1976) (in red) and Pandey et al. (2005) (in blue). There are a few stars in common among the three observations. The star #35, identified with BD+61 315, from our list is the same as the star #64 of Samson (1976) and the star # 68 of Pandey et al. (2005). While the $P\%$ measurements are found to be in agreement among all the three observations within the uncertainty, the θ_B of Pandey et al. (2005) seems to be 85° , 14° less than the value (99°) obtained by both in our measurements and by Samson (1976). A faint reflection nebulosity (Kutner *et al.* 1980; Magakian 2003) is found to be associated with BD+61 315. We suspect that, due to the lack of grid in our polarimeter, the reflection nebulosity may have contributed polarized light over the aperture used for the photometry. But, since the nebulosity is faint and no stars located along the north-south except one close to BD+61

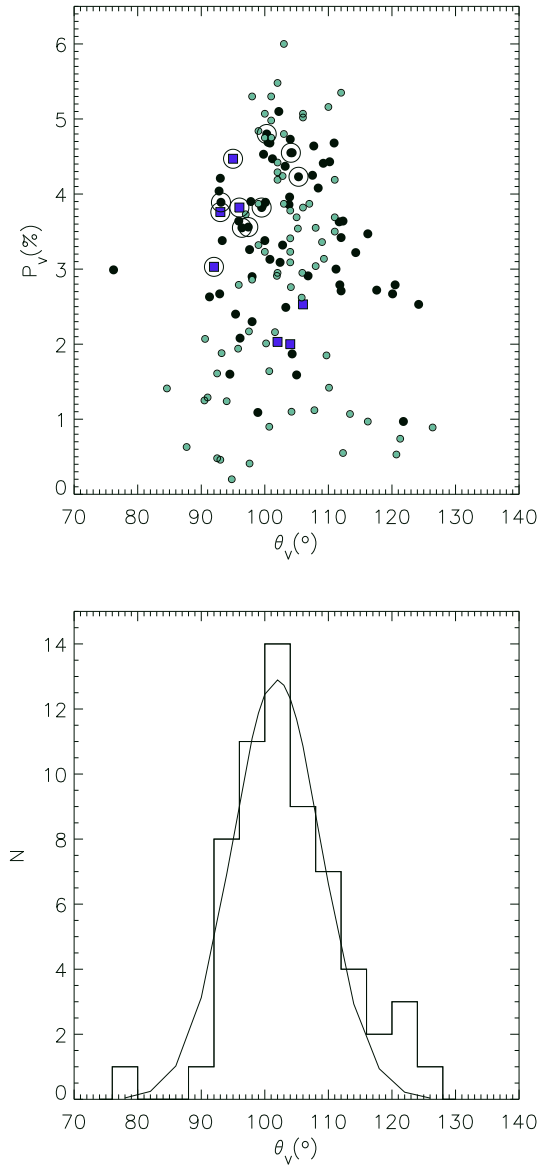


Figure 4. Upper panel: The P_V vs. θ_V plot for 61 stars observed by us in the direction of NGC 654 are shown using black filled circles. Results of stars observed by Heiles (2000) and Pandey et al. (2005) are shown using filled green circles and blue squares. The stars with $M_p \geq 0.70$ are identified using open circles. **Lower panel:** Distribution of V band position angles for the stars from our observations

315 (within $1'$), we confidently believe that none of the other stars got affected by this nebulosity. In addition to this, two other stars from our list, stars #34 & #39, are same as stars #56 & #66, respectively in Samson (1976). Both of them showed significant differences in their $P\%$ and θ_B when compared. The star #66 from Samson (1976) showed the highest polarization detected in this direction ($\sim 14 \pm 0.5\%$). Inspection of another star #1 in Samson (1976) which is same as the star #111 in Pandey et al. (2005) showed a difference of $\sim 1\%$ polarization though θ_B seems to be consistent within uncertainty.

In Figure 3, we compare our results with those obtained by Samson (1976) and Pandey

et al. (2005) using P_B vs. θ_B plot. Our results are represented by filled black circles and those of Samson (1976) and Pandey et al. (2005) are shown using filled red circles and blue squares, respectively. The results for stars observed by us are, in general, consistent with those observed by Pandey et al. (2005). But the P_B obtained by Samson (1976) are showing systematically higher values (as high as $\sim 14\%$) than those obtained in both our observations and by Pandey et al. (2005).

We used the Heiles (2000) catalogue which has a compilation of over 9000 polarization measurements to determine whether the observed polarization of stars towards the NGC 654 by us are consistent with those available in the catalogue towards the same direction. For this, we searched the catalogue for stars with polarization measurements within a circular region of radius 2° around NGC 654. We found 75 stars with polarization measurements in V band. We could not show them in Figure 1 because the nearest of them was at $\sim 17'$ ($01^h46^m03^s, +62^\circ01'03''$) away from NGC 654 ($01^h44^m00^s, +61^\circ53'06''$). In Figure 4 upper panel, we show P_V vs. θ_V plot. Our results are represented by filled black circles. The results from Pandey et al. (2005) and Heiles (2000) are represented by filled green circles and blue squares. The stars with $M_P \geq 0.70$ are identified using open circles.

The P_V of the stars observed by us are found to be in the range of ~ 1 to $\sim 5\%$. The mean value of P_V and θ_V are found to be $3.5 \pm 1\%$ and $\sim 104 \pm 9^\circ$, respectively. The stars from Heiles (2000) show degree of polarization (P_H) in the range from ~ 0.2 to $\sim 6\%$. The mean value of P_H and position angle are $\sim 3 \pm 1.7\%$ and $\sim 102^\circ \pm 9$, respectively. The range in degree of polarization and position angles obtained by us for a smaller region ($\sim 25' \times 25'$) are similar to those for a larger region from Heiles (2000) implying that the cause of polarization is possibly due to dust grains distributed in an extended structure and therefore likely to be located closer to the Sun than the cluster. A number of stars selected from Heiles (2000) show higher degree of polarization ($\gtrsim 5\%$) and among them, 5 stars are located towards the direction of NGC 663 which is found to be at a distance of ~ 2 kpc (Kharchenko et al. 2005) similar to NGC 654. Thus stars in this direction can show degree of polarization as high as $\sim 6\%$ but certainly not $\sim 14\%$ as obtained by Samson (1976). It is possible that stars which showed high polarization in Samson (1976) could be unique and definitely require further multi-wavelength investigations. Eight out of 11 stars with $M_P \geq 0.70$ are found to be clustering towards position angles which are lower than the mean value of 104° .

In Figure 4 lower panel, we show the distribution of V band position angles for stars from

our observations. The distribution is strongly peaked but shows a significant high position angle 'tail'. A Gaussian fit to the distribution is shown with peak value occurring at 102° with a dispersion in position angle of 7° . The dispersion in position angle is found to be lower in NGC 654 when compared to those for NGC 6204 and NGC 6193 (15.1° & 16° , respectively, Waldhausen *et al.* 1999) and similar to those for NGC 6611 (9.3° , Bastien *et al.* 2004), NGC 6167 (9.9° , Waldhausen *et al.* 1999), Stock 16 (6.7° , Feinstein *et al.* 2003) and IC 1805 (6.5° , Medhi *et al.* 2007). Presence of a tail in the distribution of position angles towards other clusters (e.g., NGC 6167, Waldhausen *et al.* 1999) were attributed to the dust layers located foreground to those clusters. In Figure 1 & 2 we noticed presence of opaque patches to the north of the cluster. Therefore to interpret the polarimetric results, it is important to understand the distribution of interstellar dust towards the direction of NGC 654.

3.1 Distribution of interstellar matter in the region of NGC 654

Samson (1975) noted that $E(B - V)$ for the stars in the central area of NGC 654 were lower than the stars located near the edges of the cluster. The radial increase in $E(B - V)$ was also noticed by Pandey *et al.* (2005). Samson (1975) proposed the following three possibilities to explain the decrease of $E(B - V)$; (i) the inner stars are predominantly cluster members and lie closer to us than the outer ones, (ii) a ring of obscuration lies between us and the cluster and (iii) the cluster is embedded in a shell of dust whose inner surface has a $3.6'$ diameter. He discarded the first possibility because of the knowledge of distance modulus to inner and outer stars. The second one was discarded on the basis of statistical ground arguing that its unlikely that such a ring of obscuration would lie exactly between us and NGC 654, thus favoring the third possibility of a shell around NGC 645.

Dobashi *et al.* (2005) recently produced extinction maps of the entire region of the Galaxy in the galactic latitude range $|b| \lesssim 40^\circ$ using the optical database 'Digitized Sky Survey I' and applying traditional star count technique. We obtained the fits images of the extinction map of the field containing NGC 654 from their on-line website ¹. In Figure 5 we present the high resolution extinction map overlaid with V band results from our observations and from Pandey *et al.* (2005) using vectors drawn in green and blue colours, respectively. The Figure 6 is same as Figure 5 but is overlaid with B band results from this work, Pandey

¹ <http://darkclouds.u-gakugei.ac.jp/astromer/astromer.html>

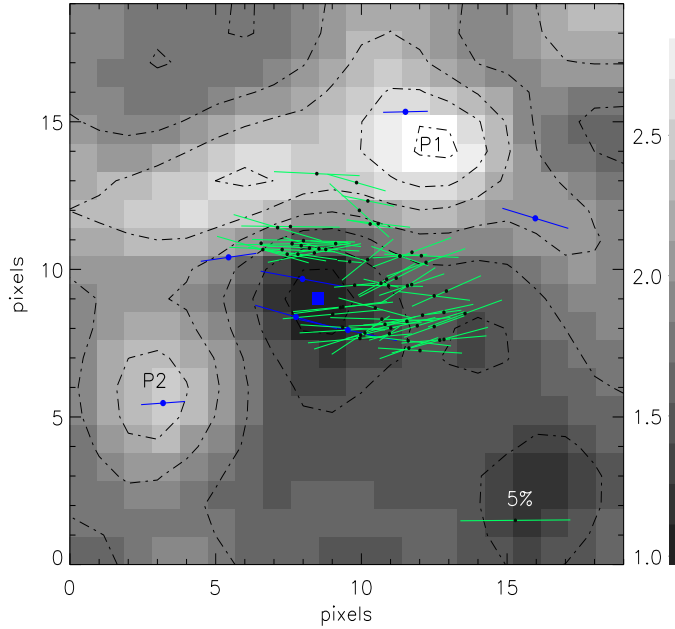


Figure 5. The high resolution extinction map of the region ($30' \times 30'$) produced by Dobashi et al. (2005) using the optical database ‘Digitized Sky Survey I’ and applying traditional star count technique. We overlay V band results from our observations and from Pandey et al. (2005) using vectors drawn in green and blue colours, respectively. Colour schemes are made different from previous figures for more clarity. The two clumps identified by Dobashi et al. (2005) in this region are identified and labeled as P1 & P2. The center of the cluster ($l = 129.08^\circ$, $b = -0.36^\circ$) is identified using blue square.

et al. (2005) and Samson (1976). Because the A_V maps shown are in galactic coordinates, we transformed all position angles measured relative to the equatorial north to the Galactic north using the relation given by Corradi et al. (1998). The square in blue colour identifies the center of the cluster ($l = 129.08^\circ$, $b = -0.36^\circ$). The colour-bar on the right shows the range of A_V values in figures. The contours are plotted at $A_V=0.5$ to 2.9 with an interval of 0.3 magnitude.

The extinction towards the location of the cluster (blue square) shows relatively low ($A_V < 1$) values. But the outer regions of the cluster especially towards the north and the east, the extinction increases up to ~ 3 magnitude. Two clumps identified by Dobashi et al. (2005) in these regions are labeled as P1 & P2 in Figures 5 & 6. Three dark clouds, LDN 1332, LDN 1334 & LDN 1337 identified towards the direction of NGC 654 are located close to P1 & P2. While LDN 1332 & LDN 1334 are found to be radially $4'$ & $7'$, respectively, away from the clump P1, LDN 1337 is found to be radially $11'$ away from the clump P2. Note that the A_V values estimated in the extinction map towards the center of the cluster are less than the values estimated by Samson (1976) & Pandey et al. (2005) by a factor of ~ 3 . This could be because of the coarse resolution of the extinction map by Dobashi et al. (2005) and the values could be an averaged one.

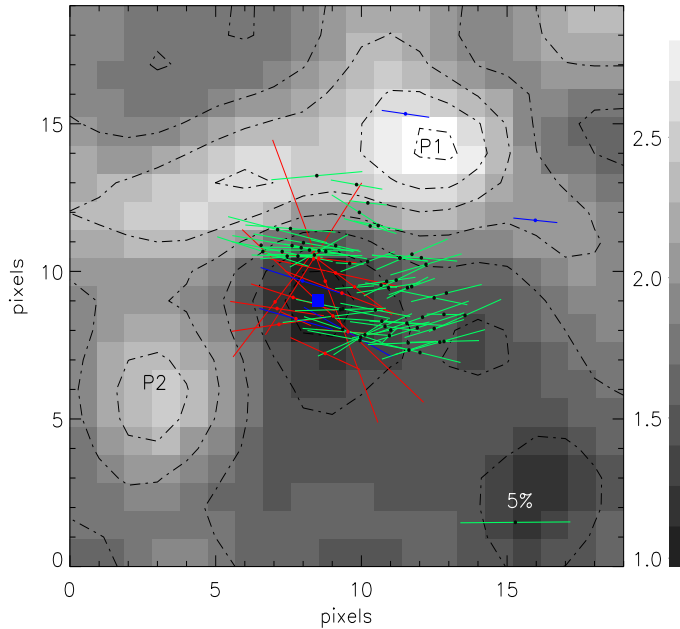


Figure 6. Same as the Figure 5 but we overlay with B band results from this work, Pandey et al. (2005) and Samson (1976). The vectors shown in red colour are the results from Samson (1976).

It is interesting to note that the overall morphology of the dust distribution in this region resembles a ring structure with a central hole coinciding with the position of the cluster. Structurally the distribution is highly inhomogeneous. This ring morphology of dust distribution explains the increase in $E(B - V)$ values found by Samson (1975) and Pandey et al. (2005) towards the edges or outer parts of the cluster. Therefore the second possibility proposed by Samson (1976) which he discarded on a statistical ground, arguing that it is unlikely that a ring of obscuration would lie exactly between us and NGC 654, seems to be the most plausible scenario. We rule out the third possibility proposed by Samson (1976), i.e., the cluster being embedded in a shell of dust, because using star count method, it would be difficult to detect dust obscurations located at ~ 2 kpc since the cloud would become inconspicuous due to the large number of foreground stars.

In order to determine distances to the foreground dust concentrations, we obtained distances and $E(B - V)$ of main sequence stars located within a circle of radius 1° around NGC 654 from the catalogue *Interstellar matter in the Galactic Disk* produced by Guarinos (1992). In Figure 7, we show the $E(B - V)$ vs. distance (pc) plot. The plot shows $E(B - V)$ increasing sharply at two distances, ~ 240 pc and ~ 1 kpc indicating that there could be at least two layers of dust one at ~ 240 pc and another at ~ 1 kpc in the direction of NGC 654. Using star counts and counts of extragalactic nebulae Heeschen (1951) also showed the

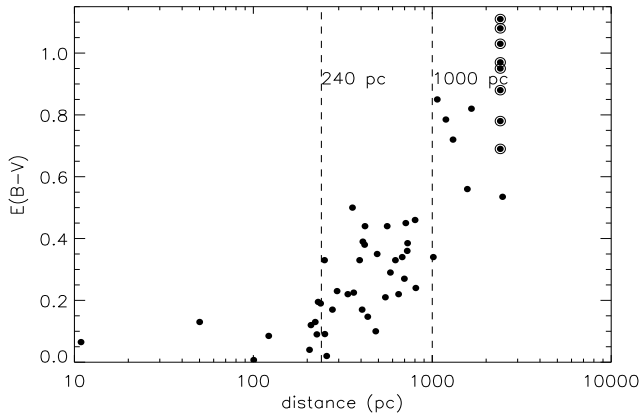


Figure 7. The distances of stars are plotted against their $E(B-V)$ from the data obtained from Guarinos (1992). The stars with $M_P \geq 0.70$ are identified using open circles. These stars are assumed to be at a distance of 2.4 kpc. The dotted lines are drawn at 240 pc and 1000 pc to show a sharp increase in $E(B-V)$ value at these distances.

presence of obscuring material at $\sim 200 - 300$ pc and at ~ 800 pc. The obscuring material located at ~ 240 pc contributes an $E(B-V) \sim 0.5$ mag while net color excess produced at 1 kpc is found to be ~ 0.85 mag. The stars with $M_P \geq 0.70$ are identified using open circles. These stars are assumed to be at a distance of 2.4 kpc. From the figure it is evident that the extinction suffered by the cluster members of ≥ 0.69 mag are mainly due to the dust layers present within 1 kpc from us.

In their photometric study of 23 open clusters, Phelps & Janes (1994) pointed out that the color-magnitude diagram of NGC 654 showed lack of the characteristic wedge-shaped distribution of the field stars. The cluster being located in front of a cloud is suggested to be the cause (Phelps & Janes 1994). The presence of a reflection nebulosity (Kutner *et al.* 1980; Magakian 2003) associated with BD+61 315 (star # 555, $M_P = 0.84$) shows that the cluster is indeed associated with a cloud. But, the relatively low $E(B-V) = 0.88$ of this star, similar to the $E(B-V)$ of 0.85 mag produced by obscuring material located at ~ 200 to 1 kpc (Figure 7), suggests that the star (also the cluster) is located just foreground to the associated cloud. This is further supported by the results of Pandey *et al.* (2005) that at the center of the cluster $E(B-V) < 1$ mag. This further strengthens the argument that the extinction towards the cluster is mainly contributed by the material distributed within 1 kpc from us. Because there is a cloud behind the cluster, the stars including those with higher membership probability observed by us, may not be background to the cloud behind the cluster. Henceforth, we believe that the observed polarization towards NGC 654 is due to the aligned dust grains associated with the clouds located at ~ 200 and $\sim 800 - 1000$ pc.

In order to investigate the polarization properties of dust grains located at different

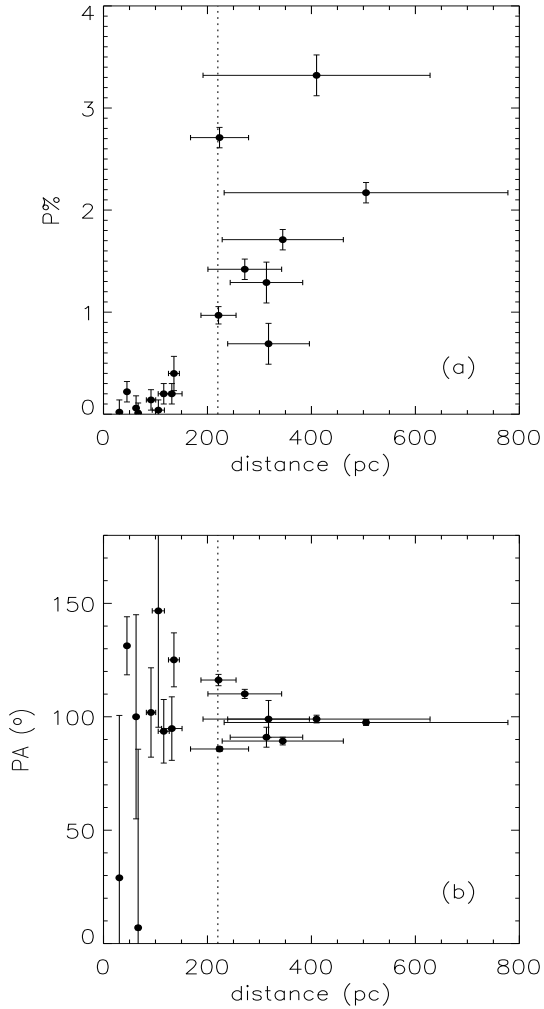


Figure 8. (a) The polarization as a function of distance is plotted. The distances are estimated from Hipparcos parallax measurements and $P\%$ values are from Heiles (2000) catalogue. (b) Position angles are plotted for same set of stars as a function of their distances.

distances from us, we selected all the stars from within a circle of radius 3° around NGC 654 for which polarization and parallax measurements are available in Heiles (2000) and the Hipparcos, respectively. The Hipparcos parallax measurements are obtained from the *Hipparcos and Tycho Catalogs*, (Perryman *et al.* 1997 and H ϕ g *et al.* 1997). We did not include the stars observed by us because of the lack of distance information for them except for the cluster member stars. Stars which showed peculiar features and emissions in their spectrum, as given by SIMBAD, are rejected.

In Figures 8 (a) and (b) we present the degree of polarization (P_{hip}) and position angle (θ_{hip}) versus distance plots, respectively. As expected, stars located closer to us show low P_{hip} ($\lesssim 0.5\%$) with a large scatter in their θ_{hip} . Stars located beyond ~ 220 pc showed relatively high values of P_{hip} in the range from 1% to 3.3% with a sharp jump in polarization ($\geq 1\%$)

occurring at ~ 220 pc. But there are no stars between ~ 150 to ~ 200 pc, so we can only infer a maximum distance to the dust grains responsible for the observed sharp jump from Figure 8. However, since the abrupt increase in both $E(B - V)$ (Figure 7) and P_{hip} (Figure 8) are found to occur at 220 – 240 pc, we assign a maximum distance of 220 pc to the first layer.

Among the two stars which showed a sharp jump in P_{hip} at ~ 220 pc, the one with higher P_{hip} (2.7%) shows a θ_{hip} of $86 \pm 1^\circ$ and the other with lower P_{hip} (1%) shows a θ_{hip} of $116 \pm 3^\circ$. Beyond ~ 220 pc, the P_{hip} increases with the distance of the stars and θ_{hip} shows less scatter as it tend to become more parallel to the Galactic plane. This implies that though majority of the dust grains in the direction of NGC 654 are aligned parallel to the Galactic plane, there are two additional population of dust grains located in the first layer at ~ 220 pc which are responsible for producing polarization with position angles both less than and greater than the Galactic parallel.

If the polarization of the starlight is caused due to the alignment of dust grains with the local magnetic field, then this implies that there exist two components of magnetic field which are responsible for the observed polarization properties. While the magnetic field component aligned more parallel with the Galactic plane is dominant towards high extinction regions, the magnetic field component which are found to be steeper than the Galactic parallel seems to be dominant towards the west and the south-west regions of NGC 654.

3.2 Serkowski Law

The maximum wavelength (λ_{max}) and the maximum polarization (P_{max}) both are functions of the optical properties and characteristic of particle size distribution of the aligned dust grains (McMillan 1978; Wilking et al. 1980). Moreover, it is also related to the interstellar extinction law (Serkowski, Mathewson & Ford 1975; Whittet & van Breda 1978; Coyne & Magalhaes 1979; Clayton & Cardelli 1988). The λ_{max} and P_{max} have been calculated by fitting the observed polarization in the B, V and R band-passes to the standard Serkowski's polarization law;

$$P_\lambda/P_{max} = \exp[-k \ln^2(\lambda_{max}/\lambda)] \quad (1)$$

and adopting the parameter $k = 1.15$ (Serkowski 1973). In the fits the degree of freedom is adopted as one. Though there are only three data points, the wavelength covered ranges from 0.44 to 0.66 μm and all the λ_{max} found to fall within this range. Since, we have enough

wavelength coverage, the fit is reasonably fine but sometimes it may cause to over estimate the value of σ_1 . For each star we computed σ_1 parameter (the unit weight error of the fit). If the polarization is well represented by the Serkowski's interstellar polarization law, σ_1 should not be higher than 1.6 due to the weighting scheme. A higher value could be indicative of the presence of intrinsic polarization. The λ_{max} can also give us the clue about the origin of polarization. The stars which have λ_{max} lower than the average value of the interstellar medium ($0.55 \pm 0.04 \mu m$, Serkowski *et al.* 1975) are the probable candidates to have an intrinsic component of polarization (Orsatti, Vega and Marraco 1998). The dispersion of the position angle ($\bar{\epsilon}$) for each star normalized by the mean value of the position angle errors is the another tool to detect the intrinsic polarization. The values obtained for P_{max} , σ_1 , λ_{max} , and $\bar{\epsilon}$ together with R.A.(2000J) and Dec(2000J) for all the 61 observed stars with their respective errors are given in Table 4.

Out of 61 observed stars three non-member stars (namely, #16, #24, and #50) and one member star (namely, #39) have the σ_1 value above the limit of 1.6. Dispersion in position angle $\bar{\epsilon}$ is higher for the member star #12 and nonmember stars #22, #24, #30, and #50. Out of these above mentioned seven probable candidates detected by using two criteria σ_1 and $\bar{\epsilon}$, the value of λ_{max} is smaller than the normal size of the grains only for the member star #12 and nonmember star #16. Although the nonmember star #16 is found to have higher value of σ_1 and lower value of λ_{max} , $\bar{\epsilon}$ is found to be very small. In the case of star #12, the value of $\bar{\epsilon}$ is high, which indicates a rotation in position angle and implies that the polarization is produced by a combination of different dust populations. Nevertheless, in majority of the observed stars, the polarization is found to be caused due to the foreground dust grains.

The weighted mean of λ_{max} for the member and nonmember stars are obtained as $0.52 \pm 0.01 \mu m$ and $0.54 \pm 0.01 \mu m$ respectively. There are not much difference of the weighted mean of λ_{max} between the member and the nonmember stars of NGC 654, which imply that the lights from the both member and nonmember stars encountering the same population of foreground dust grains. Moreover, these values are very close to the mean interstellar value of λ_{max} $0.55 \pm 0.04 \mu m$. Therefore, we can also conclude that the characteristic grain size distribution as indicated by the polarization study of stars in NGC 654 is nearly same as that for the general interstellar medium. The weighted mean of the maximum polarization for the member stars and non member stars are obtained as $3.74 \pm 0.01 \%$ and $2.87 \pm 0.01 \%$ respectively.

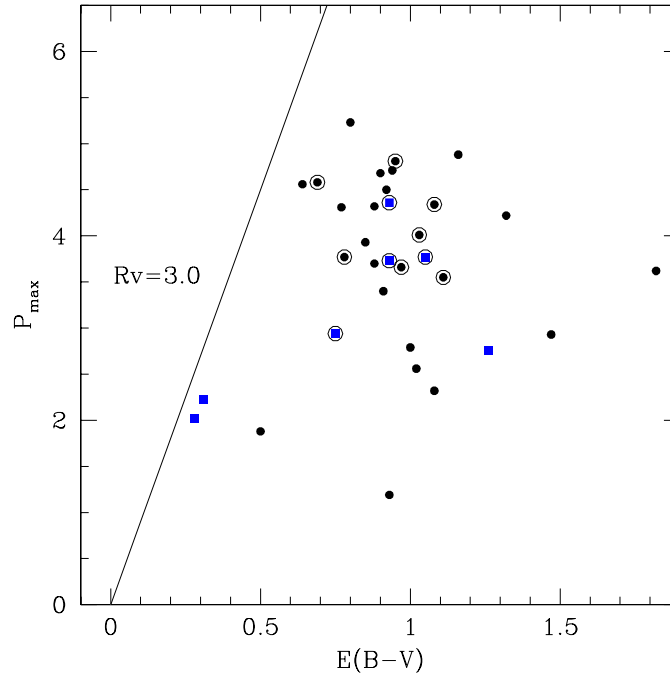


Figure 9. Polarization efficiency diagram. Using $R_V=3.0$, the line of maximum efficiency drawn. The stars observed by us in the direction of NGC 654 are shown using black filled circles. Results of stars observed by Pandey *et al.* (2005) are shown using blue squares. The stars with $M_p \geq 0.70$ are identified using open circles.

3.3 Polarization efficiency

For interstellar dust particles in diffuse interstellar medium the ratio between the maximum amount of polarization to visual extinction (polarization efficiency) can not exceed the empirical upper limit (Hiltner 1956),

$$P_{max} < 3A_V \simeq 3R_V \times E(B - V) \quad (2)$$

The ratio $P_{max}/E(B-V)$ mainly depends on the alignment efficiency, magnetic strength and the amount of depolarization due to radiation traversing more than one cloud in different direction.

Figure 9 shows the relation between colour excess $E(B - V)$ and maximum polarization P_{max} for the stars observed by us (black filled circle) and Pandey *et al.* (2005) (blue filled square) towards NGC 654 produced by the dust grains along the line of sight to the cluster. Colour excess $E(B - V)$ taken from the work of Joshi & Sagar (1983); Huestamendia *et al.* (1983). Among the 61 stars observed by us $E(B - V)$ is available only for 26 stars (8 member and 18 non-member). In the efficiency diagram none of the stars are lying to the left of the interstellar maximum line. In the previous section, though we suspect two member stars #12, #39 as a candidate for intrinsic polarization by using different criterion,

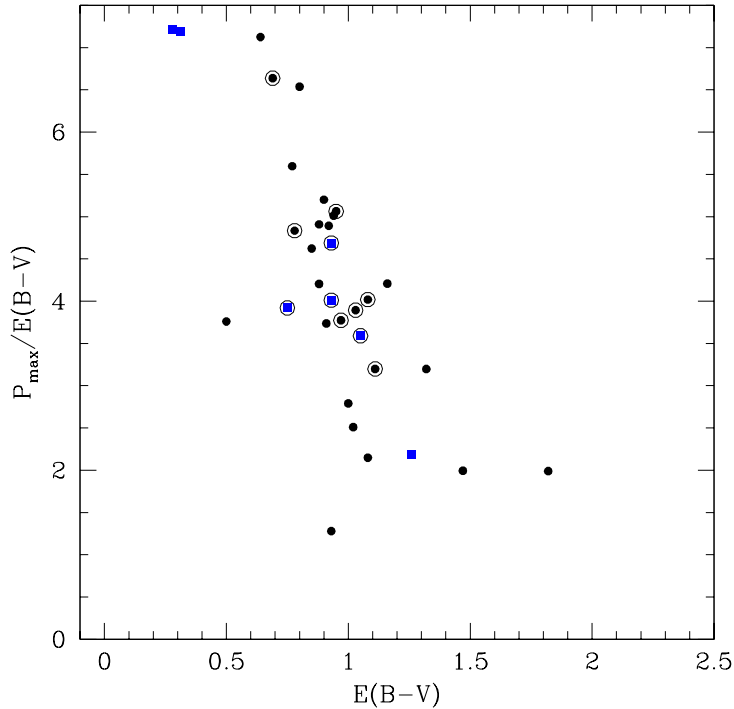


Figure 10. $P_{max}/E(B - V)$ plotted as a function of $E(B - V)$. The stars observed by us in the direction of NGC 654 are shown using black filled circles. Results of stars observed by Pandey *et al.* (2005) are shown using blue square. The stars with $M_p \geq 0.70$ are identified using open circles.

they also fall to the left in polarization efficiency diagram. From the polarization efficiency diagram it appears that apparently the stars are not affected by intrinsic polarization and the dominant mechanism of polarization for the observed member of NGC 654 is supposed to be the alignment of grains by magnetic field, like general interstellar medium. This diagram also indicates that while the colour excess for the member stars of NGC 654 varies from 0.69 to 1.11 mag approximately, the variation in the polarization value is high $\sim 1.87\%$. This high variation of P_{max} indicates the different populations of dust grains present in the line of sight towards NGC 654, as inferred from the Section 3.1.

In Figure 10, we plot the $P_{max}/E(B - V)$ vs. $E(B - V)$ for the stars observed by us and Pandey *et al.* (2005) with available colour excess $E(B - V)$. The polarization efficiency is found to fall with the increase in $E(B - V)$. There can be two possibilities for this effect (a) the dust grains are located in local cloud and the drop in efficiency is due to increase in the size of the grains; (b) the dust grains are distributed along the line of sight and the drop in efficiency is due to a slight change in the polarization position angle.

4 SUMMARY

We have observed the linear polarization for 61 stars on the region of the open cluster NGC 654. The linear polarization of the stars are caused due to the foreground dust grains. Combining our results with those from the literature and various surveys, we present evidence for the presence of at least two dust layers along the line of sight to the cluster. Their distances are estimated to be ~ 200 pc and ~ 1 kpc. Both dust layers have their local magnetic field aligned roughly parallel to the Galactic plane. From the available extinction maps, we show that the dust towards NGC 654 are distributed in a ring geometry with a hole which coincides with the center of the cluster. This explains for an increase in the extinction towards outer parts of the cluster inferred in previous studies of the region.

The weighted mean of maximum polarization P_{max} for member and nonmember stars are obtained as 3.74 ± 0.01 % and 2.87 ± 0.01 %, respectively. The weighted mean of maximum wavelength λ_{max} for the cluster members and the field stars are found to be 0.52 ± 0.01 μm and 0.54 ± 0.01 μm , respectively. These values of λ_{max} of stars towards NGC 645 are thus similar to those of ISM (0.55 ± 0.04 μm) implying that the polarization is caused mainly due to the foreground dust grains as we have inferred for IC 1805 cluster (Medhi *et al.* 2007) also in a previous study.

ACKNOWLEDGMENTS

We thank the referee for his constructive remarks which lead to great improvement in the clarity of the paper. This research has made use of the WEBDA database, operated at the Institute for Astronomy of the University of Vienna; use of image from the National Science Foundation and Digital Sky Survey (DSS), which was produced at the Space Telescope Science Institute under the US Government grant NAG W-2166; use of NASA's Astrophysics Data System and use of IRAF, distributed by National Optical Astronomy Observatories, USA. BJM thanks Orchid for her support.

REFERENCES

- Bastien, P., Mnard, F., Corporon, P., Manset, N., Poidevin, F. *et al.* , 2004, Ap&SS, 292, 427
- Clayton, G. C., Cardelli, J. A., 1988, AJ, 96, 695

- Corradi, Romano L. M., Aznar, R., Mampaso, A., 1998, MNRAS, 297, 617
- Coyne, G. V., Magalhaes, A. M., 1979, AJ, 84, 1200
- Davis, L. Jr., Greenstein, Jesse L., 1951, ApJ, 114, 206
- Dobashi, K., Uehara, H., Kandori, R., Sakurai, T., Kaiden, M., Umemoto, T., Sato, F., 2005, PASJ, 57, 1
- Feinstein, C., Baume, G., Vergne, M. M., Vazquez, R., 2003, A&A, 409, 933
- Greenberg, J. M., 1968, *Nebulae and Interstellar Matter*, ed. B.M. Middlehurst & L.H. Aller (Chicago Univ. Press), 221
- Guarinos J., 1992, *Astronomy from Large Databases II*”, ESO Conference and Workshop Proceedings No 43, ISBN 3-923524-47-1, 301
- Heeschen, David S., 1951, ApJ, 114, 132
- Heiles, Carl., 2000, AJ, 119,923
- Hiltner, W. A., 1956, ApJS, 2, 389
- Høg, E., Bässgen, G., Bastian, U., Egret, D., Fabricius, C., Großmann, V. *et al.* , 1997, A&A, 323, 57
- Huestamendia, G., del Rio, G., Mermilliod, J.C., 1993, A&AS, 100, 25
- Joshi, U. C., Sagar, Ram, 1983, MNRAS, 202, 961
- Kharchenko, N. V., Piskunov, A. E., Rser, S., Schilbach, E., Scholz, R. D., 2005, A&A, 440, 403
- Kutner, M. L., Machnik, D. E., Tucker, K. D., Dickman, R. L., 1980, ApJ, 237, 734
- Lazarian, A., Goodman, Alyssa A., Myers, Philip C., 1997, ApJ, 490, 273
- Lyngå G., 1984, *Catalogue of open clusters Data,1/1S70401*, Centre de Données Stellaires,Strasbourg.
- Magakian, T. Yu., 2003, A&A, 399, 141
- McMillan, R. S., 1978, APJ, 225, 880
- Medhi, Biman J., Maheswar, G., Brijesh, K., Pandey, J. C., Kumar, T. S., Sagar, R.,2007, MNRAS, 378, 881
- Orsatti, A. M., Vega, E., Marraco, H. G., 1998, AJ, 116, 266
- Pandey, A. K., Upadhyay, K., Ogura, K., Sagar, Ram, Mohan, V., Mito, H. *et al.* , 2005, MNRAS, 358, 1290
- Perryman, M. A. C., Lindegren, L., Kovalevsky, J., Høg, E., Bastian, U., Bernacca, P. L. *et al.* , 1997, A&A, 323, 49
- Phelps, Randy L., Janes, Kenneth A., 1994, ApJS, 90, 31

- Rautela, B. S., Joshi, G. C., Pandey, J. C., 2004, BASI, 32,159
- Sagar, Ram, Yu, Qian Zhong, 1989, MNRAS, 240, 551
- Samson, W. B., 1976, Ap&SS, 44, 217
- Samson, W. B., 1975, Ap&SS, 34, 363
- Schmidt, G. D., Elston, R., Lupie, O. L., 1992, AJ, 104, 1563
- Serkowski, K., 1973, IAUS, 52, 145
- Serkowski, K., Mathewson, D. L., Ford, V. L., 1975, ApJ, 196, 261
- Stone, R. C., 1977, A&A, 54, 803
- Waldhausen, Silvia, Martnez, Ruben E., Feinstein, Carlos, 1999, AJ, 117, 2882
- Whittet, D.C.B., van Breda, I.G., 1978, A&A, 66, 57
- Whittet, D. C. B., 1992, Dust in the Galactic Environment (Bristol:IOP)
- Wiling, B. A., Lebofsky, M. J., Kemp, J. C., Martin, P. G., Rieke, G. H., 1980, ApJ, 235, 905

This paper has been typeset from a \TeX / \LaTeX file prepared by the author.

Table 2. Observed B, V and R polarization values for different stars in NGC 654

| Sl.No. (1) | Id(P) (2) | V(mag) (3) | $P_B \pm \epsilon$ (%) (4) | $\theta_B \pm \epsilon$ ($^\circ$) (5) | $P_V \pm \epsilon$ (%) (6) | $\theta_V \pm \epsilon$ ($^\circ$) (7) | $P_R \pm \epsilon$ (%) (8) | $\theta_R \pm \epsilon$ ($^\circ$) (9) | E_{B-V} (10) | M_p (11) |
|---------------|--------------|---------------|-------------------------------|---|-------------------------------|---|-------------------------------|---|-------------------|---------------|
| 01 | — | 16.66 | 3.37 \pm 0.56 | 114 \pm 5 | 3.42 \pm 0.25 | 112 \pm 2 | 3.47 \pm 0.27 | 108 \pm 2 | — | — |
| 02 | — | 16.16 | 3.23 \pm 0.30 | 109 \pm 3 | 3.22 \pm 0.02 | 114 \pm 2 | 3.20 \pm 0.18 | 116 \pm 2 | — | — |
| 03 | — | 15.17 | 1.57 \pm 0.08 | 101 \pm 2 | 1.59 \pm 0.05 | 105 \pm 1 | 1.57 \pm 0.07 | 101 \pm 4 | — | — |
| 04 | — | 17.05 | 3.18 \pm 0.14 | 102 \pm 1 | 3.86 \pm 0.26 | 104 \pm 2 | 3.35 \pm 0.13 | 105 \pm 2 | — | — |
| 05 | — | 16.71 | 4.15 \pm 0.65 | 110 \pm 5 | 4.41 \pm 0.13 | 109 \pm 1 | 4.10 \pm 0.53 | 112 \pm 4 | — | — |
| 06 | — | 14.96 | 2.73 \pm 0.10 | 110 \pm 1 | 2.79 \pm 0.05 | 112 \pm 1 | 2.49 \pm 0.06 | 111 \pm 1 | — | — |
| 07 | — | 17.65 | 3.03 \pm 0.37 | 95 \pm 4 | 3.26 \pm 0.40 | 98 \pm 4 | 3.12 \pm 0.07 | 101 \pm 2 | — | — |
| 08 | — | 15.99 | 3.28 \pm 0.36 | 110 \pm 3 | 3.63 \pm 0.01 | 112 \pm 1 | 3.49 \pm 0.04 | 109 \pm 1 | — | — |
| 09 | — | 16.68 | 3.26 \pm 0.49 | 99 \pm 4 | 3.38 \pm 0.28 | 100 \pm 2 | 3.38 \pm 0.28 | 100 \pm 2 | — | — |
| 10 | — | 17.35 | 3.31 \pm 0.50 | 114 \pm 4 | 3.64 \pm 0.33 | 112 \pm 3 | 3.79 \pm 0.86 | 115 \pm 7 | — | — |
| 11 | — | 16.62 | 4.27 \pm 0.13 | 112 \pm 1 | 4.64 \pm 0.27 | 108 \pm 2 | 4.69 \pm 0.12 | 112 \pm 1 | — | — |
| 12 | 703 | 13.11 | 3.71 \pm 0.07 | 94 \pm 1 | 3.82 \pm 0.18 | 100 \pm 2 | 3.41 \pm 0.01 | 93 \pm 1 | 0.78 | 0.70 |
| 13 | — | 14.93 | 4.33 \pm 0.04 | 111 \pm 1 | 4.43 \pm 0.05 | 110 \pm 1 | 4.09 \pm 0.17 | 108 \pm 1 | — | — |
| 14 | — | 14.74 | 2.49 \pm 0.07 | 111 \pm 1 | 2.71 \pm 0.18 | 112 \pm 2 | 2.39 \pm 0.04 | 111 \pm 1 | — | — |
| 15 | — | 16.98 | 3.66 \pm 0.37 | 103 \pm 4 | 3.90 \pm 0.64 | 98 \pm 5 | 3.51 \pm 0.29 | 104 \pm 2 | — | — |
| 16 | — | 16.96 | 3.41 \pm 0.27 | 100 \pm 4 | 3.96 \pm 0.08 | 104 \pm 1 | 3.52 \pm 0.05 | 104 \pm 1 | — | — |
| 17 | — | 16.20 | 2.13 \pm 0.36 | 112 \pm 5 | 3.00 \pm 0.45 | 111 \pm 4 | 2.23 \pm 0.11 | 109 \pm 2 | — | — |
| 18 | — | 17.28 | 1.95 \pm 0.66 | 117 \pm 10 | 2.67 \pm 0.36 | 120 \pm 2 | 2.25 \pm 0.10 | 125 \pm 1 | — | — |
| 19 | — | 15.68 | 2.54 \pm 0.18 | 98 \pm 2 | 2.49 \pm 0.21 | 103 \pm 2 | 2.36 \pm 0.11 | 97 \pm 2 | — | — |
| 20 | — | 16.08 | 2.55 \pm 0.19 | 98 \pm 2 | 2.63 \pm 0.13 | 91 \pm 1 | 2.47 \pm 0.11 | 97 \pm 2 | — | — |
| 21 | — | 16.19 | 3.04 \pm 0.09 | 116 \pm 1 | 3.47 \pm 0.25 | 116 \pm 2 | 3.01 \pm 0.19 | 109 \pm 2 | — | — |
| 22 | — | 15.71 | 2.91 \pm 0.11 | 106 \pm 1 | 3.13 \pm 0.02 | 101 \pm 1 | 2.98 \pm 0.02 | 100 \pm 1 | — | — |
| 23 | — | 15.75 | 2.62 \pm 0.33 | 106 \pm 4 | 2.72 \pm 0.20 | 118 \pm 2 | 2.71 \pm 0.24 | 109 \pm 3 | — | — |
| 24 | — | 15.86 | 1.45 \pm 0.02 | 97 \pm 1 | 1.60 \pm 0.03 | 95 \pm 1 | 1.33 \pm 0.10 | 104 \pm 2 | — | — |
| 25 | — | 16.05 | 3.54 \pm 0.38 | 108 \pm 3 | 4.08 \pm 0.34 | 108 \pm 3 | 3.44 \pm 0.10 | 107 \pm 1 | — | — |
| 26 | — | 15.54 | 0.75 \pm 0.02 | 129 \pm 1 | 0.97 \pm 0.20 | 122 \pm 6 | 0.79 \pm 0.09 | 128 \pm 4 | — | — |
| 27 | — | 15.94 | 3.19 \pm 0.10 | 97 \pm 1 | 3.32 \pm 0.30 | 103 \pm 3 | 3.17 \pm 0.03 | 102 \pm 1 | — | — |
| 28 | — | 17.33 | 4.26 \pm 0.01 | 100 \pm 1 | 4.69 \pm 0.89 | 101 \pm 5 | 3.90 \pm 1.39 | 95 \pm 10 | — | — |
| 29 | 530 | 16.84 | 2.51 \pm 0.39 | 112 \pm 4 | 2.53 \pm 0.03 | 124 \pm 1 | 2.31 \pm 0.48 | 121 \pm 7 | 1.02 | — |
| 30 | 648 | 15.69 | 3.19 \pm 0.06 | 96 \pm 1 | 3.38 \pm 0.04 | 93 \pm 1 | 3.30 \pm 0.03 | 91 \pm 1 | 0.91 | — |
| 31 | 641 | 16.06 | 4.39 \pm 0.03 | 115 \pm 1 | 4.68 \pm 0.26 | 111 \pm 2 | 4.10 \pm 0.17 | 116 \pm 1 | 0.92 | — |
| 32 | 642 | 16.87 | 2.61 \pm 0.44 | 120 \pm 5 | 2.79 \pm 0.07 | 121 \pm 1 | 2.65 \pm 0.20 | 121 \pm 3 | 1.00 | — |
| 33 | 637 | 17.52 | 4.79 \pm 0.41 | 96 \pm 2 | 4.73 \pm 0.22 | 104 \pm 1 | 4.78 \pm 0.12 | 100 \pm 1 | 1.16 | — |
| 34 | 493 | 13.78 | 1.77 \pm 0.01 | 104 \pm 1 | 1.87 \pm 0.01 | 104 \pm 3 | 1.83 \pm 0.01 | 100 \pm 1 | 0.50 | 0.00 |
| 35 | 555 | 10.74 | 4.10 \pm 0.07 | 99 \pm 1 | 4.37 \pm 0.09 | 103 \pm 1 | 4.12 \pm 0.02 | 101 \pm 1 | 0.88 | 0.84 |
| 36 | 634 | 16.33 | 3.57 \pm 0.12 | 92 \pm 1 | 3.84 \pm 0.26 | 100 \pm 2 | 3.15 \pm 0.13 | 98 \pm 1 | 1.82 | — |
| 37 | 450 | 12.86 | 4.28 \pm 0.31 | 95 \pm 2 | 4.55 \pm 0.03 | 104 \pm 1 | 4.23 \pm 0.22 | 102 \pm 1 | 0.64 | 0.55 |
| 38 | 439 | 14.53 | 4.13 \pm 0.06 | 102 \pm 5 | 4.23 \pm 0.08 | 105 \pm 1 | 4.17 \pm 0.01 | 107 \pm 2 | 1.08 | 0.89 |
| 39 | 556 | 12.86 | 4.56 \pm 0.11 | 105 \pm 1 | 4.55 \pm 0.03 | 104 \pm 1 | 4.35 \pm 0.01 | 105 \pm 1 | 0.69 | 0.90 |
| 40 | — | 15.67 | 2.23 \pm 0.50 | 96 \pm 6 | 2.90 \pm 0.15 | 98 \pm 2 | 2.48 \pm 0.13 | 99 \pm 2 | — | — |
| 41 | — | 15.96 | 2.41 \pm 0.29 | 93 \pm 3 | 2.08 \pm 0.36 | 96 \pm 5 | 2.30 \pm 0.08 | 99 \pm 1 | — | — |
| 42 | — | 16.53 | 2.65 \pm 0.49 | 83 \pm 5 | 2.99 \pm 0.40 | 76 \pm 3 | 2.43 \pm 0.13 | 88 \pm 2 | — | — |
| 43 | — | 16.84 | 1.72 \pm 0.35 | 98 \pm 6 | 2.40 \pm 0.56 | 95 \pm 7 | 2.04 \pm 0.11 | 98 \pm 2 | — | — |
| 44 | — | 16.38 | 2.35 \pm 0.58 | 96 \pm 7 | 2.67 \pm 0.15 | 93 \pm 3 | 2.54 \pm 0.20 | 100 \pm 2 | — | — |
| 45 | 474 | 14.87 | 1.27 \pm 0.20 | 100 \pm 5 | 1.09 \pm 0.11 | 99 \pm 3 | 1.15 \pm 0.04 | 94 \pm 1 | 0.93 | — |
| 46 | 405 | 16.51 | 2.28 \pm 0.10 | 95 \pm 1 | 2.30 \pm 0.09 | 98 \pm 4 | 1.97 \pm 0.25 | 103 \pm 4 | 1.08 | — |
| 47 | 322 | 15.51 | 3.78 \pm 0.17 | 96 \pm 2 | 3.89 \pm 0.26 | 93 \pm 3 | 3.91 \pm 0.16 | 95 \pm 2 | 1.03 | 0.86 |
| 48 | 267 | 16.72 | 2.76 \pm 0.43 | 118 \pm 5 | 2.91 \pm 0.11 | 107 \pm 1 | 2.62 \pm 0.18 | 110 \pm 2 | 1.47 | — |
| 49 | — | 16.19 | 4.14 \pm 0.37 | 104 \pm 3 | 3.89 \pm 0.35 | 100 \pm 1 | 3.83 \pm 0.40 | 101 \pm 3 | — | — |
| 50 | 238 | 14.93 | 4.35 \pm 0.20 | 101 \pm 1 | 4.25 \pm 0.04 | 108 \pm 1 | 4.26 \pm 0.01 | 101 \pm 1 | 0.77 | 0.03 |
| 51 | 187 | 16.20 | 4.48 \pm 0.03 | 102 \pm 1 | 4.53 \pm 0.18 | 100 \pm 1 | 4.44 \pm 0.01 | 97 \pm 2 | 0.90 | — |
| 52 | 150 | 17.26 | 4.57 \pm 0.17 | 96 \pm 1 | 4.68 \pm 0.46 | 100 \pm 3 | 4.40 \pm 0.04 | 103 \pm 1 | 0.94 | 0.11 |
| 53 | 132 | 15.93 | 3.58 \pm 0.12 | 101 \pm 1 | 3.09 \pm 0.48 | 102 \pm 4 | 3.50 \pm 0.09 | 97 \pm 1 | 0.88 | — |
| 54 | 119 | 17.39 | 3.44 \pm 0.61 | 104 \pm 5 | 3.56 \pm 0.62 | 97 \pm 5 | 3.57 \pm 0.15 | 94 \pm 1 | 0.97 | 0.95 |
| 55 | 080 | 17.18 | 5.45 \pm 0.45 | 97 \pm 11 | 5.10 \pm 0.15 | 102 \pm 2 | 4.80 \pm 0.10 | 92 \pm 2 | 0.80 | 0.11 |
| 56 | — | 16.80 | 4.10 \pm 0.69 | 99 \pm 5 | 4.47 \pm 1.08 | 101 \pm 12 | 4.01 \pm 0.31 | 102 \pm 2 | — | — |
| 57 | 061 | 16.63 | 3.23 \pm 0.46 | 101 \pm 15 | 3.55 \pm 0.29 | 96 \pm 1 | 3.46 \pm 0.47 | 95 \pm 4 | 1.11 | 0.83 |
| 58 | 034 | 16.75 | 4.61 \pm 0.61 | 96 \pm 3 | 4.80 \pm 0.17 | 100 \pm 1 | 4.53 \pm 0.10 | 99 \pm 1 | 0.95 | 0.90 |
| 59 | — | 15.74 | 4.54 \pm 0.46 | 94 \pm 3 | 4.04 \pm 0.24 | 93 \pm 2 | 4.12 \pm 0.15 | 92 \pm 1 | — | — |
| 60 | 562 | 14.70 | 4.21 \pm 0.20 | 92 \pm 1 | 4.21 \pm 0.03 | 93 \pm 1 | 4.12 \pm 0.15 | 92 \pm 1 | 1.32 | — |
| 61 | 563 | 15.60 | 4.12 \pm 0.55 | 96 \pm 1 | 3.64 \pm 0.34 | 96 \pm 3 | 3.72 \pm 0.07 | 93 \pm 1 | 0.85 | — |

Table 3. Results of previous polarization measurements carried out by Samson (1976) and Pandey et al. (2005) in the direction of NGC 654. The errors in the measurements are given in parenthesis.

| Id | P_B (%) | θ_B ($^\circ$) | P_V (%) | θ_V ($^\circ$) | P_R (%) | θ_R ($^\circ$) | P_I (%) | θ_I ($^\circ$) | M_P (%) |
|----------------------|--------------|----------------------------|--------------|----------------------------|--------------|----------------------------|--------------|----------------------------|--------------|
| (1) | (2) | (3) | (4) | (5) | (6) | (7) | (8) | (9) | (10) |
| Samson (1976) | | | | | | | | | |
| 1 | 2.12 (1.0) | 88 | — | — | — | — | — | — | 0.86 |
| 5 | 6.45 (2.8) | 106 | — | — | — | — | — | — | 0.92 |
| 8 | 6.95 (4.7) | 136 | — | — | — | — | — | — | 0.92 |
| 9 | 6.40 (2.3) | 97 | — | — | — | — | — | — | 0.91 |
| 14 | 5.80 (2.9) | 92 | — | — | — | — | — | — | 0.82 |
| 36 | 5.16 (1.0) | 98 | — | — | — | — | — | — | 0.90 |
| 37 | 8.52 (0.4) | 141 | — | — | — | — | — | — | 0.92 |
| 40 | 12.39 (5.3) | 47 | — | — | — | — | — | — | 0.87 |
| 41 | 9.03 (1.2) | 95 | — | — | — | — | — | — | 0.82 |
| 54 | 7.97 (3.1) | 90 | — | — | — | — | — | — | 0.93 |
| 56 | 5.48 (1.7) | 80 | — | — | — | — | — | — | 0.00 |
| 64 | 4.37 (1.7) | 99 | — | — | — | — | — | — | 0.84 |
| 65 | 4.88 (2.0) | 88 | — | — | — | — | — | — | 0.89 |
| 66 | 13.82 (0.5) | 75 | — | — | — | — | — | — | 0.90 |
| Pandey et al. (2005) | | | | | | | | | |
| 9 | 2.00(0.47) | 98(7) | 3.03(0.16) | 92(2) | 2.68(0.11) | 94(1) | 2.31(0.17) | 98(2) | 0.92 |
| 57 | 2.16(0.36) | 97(5) | 2.03(0.15) | 102(2) | 1.48(0.14) | 98(3) | 1.25(0.26) | 97(5) | 0.90 |
| 68 | 4.18(0.70) | 85(5) | 4.47(0.19) | 95(1) | 3.78(0.11) | 94(1) | 3.42(0.18) | 95(2) | 0.84 |
| 109 | 3.86(0.22) | 92(2) | 3.82(0.06) | 96(1) | 3.23(0.05) | 96(1) | 3.00(0.07) | 95(1) | 0.90 |
| 111 | 3.37(0.26) | 93(2) | 3.76(0.09) | 93(1) | 3.32(0.06) | 93(1) | 2.78(0.08) | 93(1) | 0.86 |
| 137 | — | — | 2.53(0.32) | 106(4) | 2.03(0.18) | 114(3) | 1.51(0.29) | 111(6) | 0.00 |
| 161 | — | — | 2.00(0.21) | 104(3) | 1.94(0.17) | 110(2) | 1.81(0.29) | 103(5) | 0.48 |

Table 4. The P_{max} , λ_{max} , σ_1 & $\bar{\tau}$ for the observed data in NGC 654.

| Sl.No. | R.A(2000J) | DEC(2000J) | $P_{max} \pm \epsilon$ (%) | σ_1 | $\lambda_{max} \pm \epsilon$ (μm) | $\bar{\tau}$ |
|--------|-------------|------------|----------------------------|------------|--|--------------|
| 01 | 01 42 39.54 | 61 51 18.4 | 3.50 \pm 0.08 | 0.43 | 0.58 \pm 0.05 | 0.81 |
| 02 | 01 42 49.68 | 61 52 50.9 | 3.22 \pm 0.02 | 0.83 | 0.56 \pm 0.05 | 1.32 |
| 03 | 01 42 51.02 | 61 51 19.4 | 1.62 \pm 0.01 | 0.74 | 0.54 \pm 0.03 | 0.92 |
| 04 | 01 42 51.00 | 61 49 23.4 | 3.49 \pm 0.15 | 1.55 | 0.57 \pm 0.05 | 0.56 |
| 05 | 01 42 53.27 | 61 49 20.5 | 4.41 \pm 0.13 | 0.20 | 0.53 \pm 0.02 | 0.44 |
| 06 | 01 42 56.33 | 61 50 18.7 | 2.81 \pm 0.05 | 0.93 | 0.48 \pm 0.02 | 1.06 |
| 07 | 01 42 56.36 | 61 52 30.2 | 3.23 \pm 0.01 | 0.08 | 0.55 \pm 0.01 | 0.66 |
| 08 | 01 43 00.81 | 61 55 00.8 | 3.63 \pm 0.01 | 0.42 | 0.55 \pm 0.01 | 0.58 |
| 09 | 01 43 03.34 | 61 55 29.5 | 3.44 \pm 0.05 | 0.26 | 0.57 \pm 0.03 | 0.22 |
| 10 | 01 43 08.45 | 61 55 44.4 | 3.71 \pm 0.07 | 0.15 | 0.61 \pm 0.03 | 0.21 |
| 11 | 01 43 02.69 | 61 51 07.4 | 4.74 \pm 0.12 | 0.25 | 0.60 \pm 0.01 | 2.21 |
| 12 | 01 43 04.08 | 61 48 35.7 | 3.77 \pm 0.03 | 0.59 | 0.49 \pm 0.01 | 4.35 |
| 13 | 01 43 05.56 | 61 50 21.9 | 4.45 \pm 0.11 | 0.29 | 0.51 \pm 0.01 | 1.78 |
| 14 | 01 43 10.11 | 61 48 46.3 | 2.57 \pm 0.04 | 0.86 | 0.51 \pm 0.02 | 0.33 |
| 15 | 01 43 10.51 | 61 49 17.4 | 3.79 \pm 0.05 | 0.22 | 0.51 \pm 0.02 | 0.64 |
| 16 | 01 43 11.22 | 61 50 41.3 | 3.93 \pm 0.24 | 2.14 | 0.49 \pm 0.05 | 1.09 |
| 17 | 01 43 08.59 | 61 53 18.5 | 2.39 \pm 0.02 | 1.46 | 0.52 \pm 0.13 | 0.28 |
| 18 | 01 43 10.91 | 61 53 13.8 | 2.42 \pm 0.03 | 0.95 | 0.52 \pm 0.12 | 0.72 |
| 19 | 01 43 15.02 | 61 55 28.1 | 2.57 \pm 0.03 | 0.28 | 0.50 \pm 0.01 | 1.20 |
| 20 | 01 43 15.03 | 61 55 28.2 | 2.64 \pm 0.01 | 0.03 | 0.52 \pm 0.01 | 1.63 |
| 21 | 01 43 17.03 | 61 53 46.4 | 3.22 \pm 0.11 | 1.09 | 0.55 \pm 0.04 | 2.01 |
| 22 | 01 43 21.23 | 61 53 13.6 | 3.13 \pm 0.01 | 0.71 | 0.54 \pm 0.01 | 4.63 |
| 23 | 01 43 22.23 | 61 53 41.2 | 2.76 \pm 0.04 | 0.27 | 0.56 \pm 0.02 | 1.68 |
| 24 | 01 43 25.32 | 61 53 24.8 | 1.57 \pm 0.01 | 2.29 | 0.57 \pm 0.05 | 3.23 |
| 25 | 01 43 20.00 | 61 50 12.4 | 3.79 \pm 0.27 | 1.11 | 0.50 \pm 0.06 | 0.26 |
| 26 | 01 43 20.74 | 61 49 48.3 | 0.82 \pm 0.05 | 0.78 | 0.58 \pm 0.05 | 0.84 |
| 27 | 01 43 23.13 | 61 50 28.0 | 3.33 \pm 0.01 | 0.04 | 0.54 \pm 0.01 | 1.77 |
| 28 | 01 43 24.85 | 61 50 50.4 | 4.45 \pm 0.19 | 0.36 | 0.54 \pm 0.05 | 0.45 |
| 29 | 01 43 32.36 | 61 55 12.7 | 2.56 \pm 0.01 | 0.05 | 0.50 \pm 0.01 | 1.15 |
| 30 | 01 43 28.43 | 61 51 38.5 | 3.40 \pm 0.01 | 0.49 | 0.56 \pm 0.01 | 3.49 |
| 31 | 01 43 34.08 | 61 49 51.6 | 4.50 \pm 0.16 | 0.89 | 0.51 \pm 0.02 | 2.00 |
| 32 | 01 43 36.39 | 61 49 41.9 | 2.79 \pm 0.01 | 0.13 | 0.54 \pm 0.01 | 0.15 |
| 33 | 01 43 36.81 | 61 49 27.9 | 4.88 \pm 0.12 | 0.94 | 0.57 \pm 0.04 | 1.80 |
| 34 | 01 43 39.68 | 61 53 15.9 | 1.88 \pm 0.01 | 1.53 | 0.56 \pm 0.01 | 1.56 |
| 35 | 01 43 43.51 | 61 50 03.5 | 4.32 \pm 0.05 | 0.64 | 0.54 \pm 0.02 | 1.42 |
| 36 | 01 43 46.18 | 61 50 14.9 | 3.62 \pm 0.12 | 1.26 | 0.48 \pm 0.03 | 2.17 |
| 37 | 01 43 46.03 | 61 51 42.9 | 4.56 \pm 0.15 | 0.48 | 0.53 \pm 0.02 | 2.70 |
| 38 | 01 43 47.45 | 61 51 40.1 | 4.34 \pm 0.04 | 1.41 | 0.55 \pm 0.08 | 0.66 |
| 39 | 01 43 51.62 | 61 51 11.3 | 4.58 \pm 0.05 | 1.78 | 0.53 \pm 0.01 | 1.13 |
| 40 | 01 43 26.83 | 61 57 40.2 | 2.84 \pm 0.13 | 1.46 | 0.48 \pm 0.10 | 0.36 |
| 41 | 01 43 31.24 | 61 57 38.3 | 2.41 \pm 0.15 | 0.98 | 0.53 \pm 0.07 | 0.67 |
| 42 | 01 43 37.10 | 61 58 36.8 | 2.83 \pm 0.28 | 0.74 | 0.47 \pm 0.06 | 1.46 |
| 43 | 01 43 32.48 | 61 59 17.4 | 2.06 \pm 0.08 | 0.71 | 0.62 \pm 0.09 | 0.23 |
| 44 | 01 43 38.64 | 62 00 36.0 | 2.65 \pm 0.04 | 0.30 | 0.55 \pm 0.03 | 0.65 |
| 45 | 01 43 42.38 | 61 54 57.3 | 1.19 \pm 0.08 | 1.17 | 0.55 \pm 0.01 | 0.93 |
| 46 | 01 43 50.02 | 61 56 14.3 | 2.32 \pm 0.04 | 0.52 | 0.49 \pm 0.02 | 1.00 |
| 47 | 01 43 55.40 | 61 55 49.5 | 4.01 \pm 0.05 | 0.51 | 0.56 \pm 0.07 | 0.57 |
| 48 | 01 43 59.12 | 61 55 52.2 | 2.93 \pm 0.07 | 0.40 | 0.49 \pm 0.03 | 1.68 |
| 49 | 01 44 00.30 | 62 01 14.3 | 4.11 \pm 0.15 | 0.58 | 0.49 \pm 0.04 | 0.84 |
| 50 | 01 44 01.63 | 61 55 34.3 | 4.31 \pm 0.05 | 2.46 | 0.59 \pm 0.03 | 4.16 |
| 51 | 01 44 04.29 | 61 55 55.1 | 4.68 \pm 0.11 | 0.78 | 0.53 \pm 0.01 | 1.66 |
| 52 | 01 44 07.58 | 61 56 26.9 | 4.71 \pm 0.01 | 0.02 | 0.52 \pm 0.01 | 1.84 |
| 53 | 01 44 08.81 | 61 56 05.5 | 3.70 \pm 0.10 | 1.27 | 0.53 \pm 0.03 | 1.32 |
| 54 | 01 44 10.59 | 61 55 29.3 | 3.66 \pm 0.01 | 0.17 | 0.57 \pm 0.07 | 0.97 |
| 55 | 01 44 13.77 | 61 56 14.1 | 5.23 \pm 0.17 | 0.88 | 0.50 \pm 0.03 | 0.71 |
| 56 | 01 44 14.67 | 61 57 27.4 | 4.28 \pm 0.08 | 0.20 | 0.52 \pm 0.02 | 0.16 |
| 57 | 01 44 16.44 | 61 55 29.1 | 3.55 \pm 0.02 | 0.08 | 0.58 \pm 0.08 | 0.35 |
| 58 | 01 44 19.17 | 61 55 48.8 | 4.81 \pm 0.06 | 0.05 | 0.53 \pm 0.01 | 0.96 |
| 59 | 01 44 21.67 | 61 57 23.0 | 4.29 \pm 0.27 | 1.42 | 0.53 \pm 0.08 | 0.33 |
| 60 | 01 44 29.70 | 61 55 48.9 | 4.22 \pm 0.04 | 1.14 | 0.53 \pm 0.04 | 0.43 |
| 61 | 01 44 30.64 | 61 56 15.9 | 3.93 \pm 0.26 | 1.04 | 0.53 \pm 0.07 | 0.87 |